Available online at www.sciencedirect.com
SCIENCE DIRECT®
Journal of the European Ceramic Society 26 (2006) 351–359
www.elsevier.com/locate/jeurceramsoc

Scratch behavior of SiAlON ceramics

Ramasamy Sivakumar[1], Mark I. Jones, Kiyoshi Hirao, Wataru Kanematsu*

National Institute of Advanced Industrial Science and Technology (AIST), 2266-98 Shimo Shidami, Moriyama-ku, Nagoya 463-8560, Japan

Received 26 June 2004; received in revised form 15 November 2004; accepted 21 November 2004
Available online 21 January 2005

Abstract

The mechanical response of four different types of hot pressed yttrium stabilized α/β composite SiAlON ceramics was investigated by scratch testing in order to interpret their severe wear behavior. A progressive loading scratch tester with both rough and smooth spherical diamond styluses was used to analyze the variation in mechanical response with roughness of stylus. The extent of subsurface damage produced by the different styluses on a 50% β-content composite was also investigated using a visualization technique with plasma etching, which has been previously developed by one of the authors. When scratched by the rough stylus, quasi-plastic deformation recognized in the form of grain release after plasma etching was present predominantly in the surface, and the use of this stylus was regarded to be more appropriate for comparing the results of scratch tests with those of severe wear due to similarity of crack formation between grain dislodgement in severe wear and subsurface damage in the scratch tests. The work required to produce damage and groove formation (W_{dg}) when scratched by the rough stylus was evaluated for all test materials and it was found that the worn volume under severe wear follows the reverse order of W_{dg}.

Keywords: Sialon; Microstructure-final; Fracture; Wear resistance; Scratch test

1. Introduction

Non-oxide ceramics are widely used in various tribological applications due to their excellent mechanical properties, such as high strength, high hardness and chemical stability at high temperatures. Elaborate studies have been performed in order to understand their wear properties.[1–13] Wear in ceramics is a complicated process due to the contribution of test conditions, such as normal load,[6] sliding velocity,[7] as well as humidity[8–10] and temperature[11–13] of the testing atmosphere. In general, wear can be broadly classified into two categories; mild and severe wear, which occurs mainly due to low and high contact stresses, respectively. Severe wear is dominated by brittle fracture and is associated with high wear rates,[14] whereas mild wear is dominated by tribochemical reactions and lower wear rates.[2]

Scratch testing is an appropriate technique that provides more fundamental information on wear mechanisms and is used to simulate the fracture in sliding wear. In particular, scratches by progressive loading,[15] that is, increasing the load with scratch distance can be useful to investigate changing damage patterns in a single scratch. During scratch testing, subsurface damage is generated beneath the sliding contact. A commonly used sectioning technique to detect the subsurface damage is the bonded interface technique, where sections cut perpendicular to the scratch direction previously bonded by adhesive are viewed by scanning electron microscope (SEM).[16] However, this technique does not lend itself to visualization of shallow subsurface damage occurring under low normal loads. The technique of taper-sectioning of scratched specimens followed by plasma etching[17] is used in this work, where the presence of shallow damage simulating the actual wear can be readily identified. The advantage of plasma etching is that it enhances the view of cracks and the subsurface intergranular microcracking zone known as the quasi-plastic deformation zone in the form of grain release. It is assumed that the grain release is due to preferential etching, by plasma

* Corresponding author. Tel.: +81 52 736 7220; fax: +81 52 736 7224.
E-mail address: w.kanematsu@aist.go.jp (W. Kanematsu).
[1] Present address: National Institute for Materials Science, Tsukuba, Japan.

0955-2219/$ – see front matter © 2004 Elsevier Ltd. All rights reserved.
doi:10.1016/j.jeurceramsoc.2004.11.010

Table 1
Mechanical properties of test materials

Material	m	n	Calculated β-content (%)	Vickers hardness (%)	Fracture toughness ($MPam^{1/2}$)	4pt-Bending strength (MPa)
A	0.5	0.25	49	19.46	4.97	885
B	0.7	0.35	25	19.64	4.43	720
C	1.0	0.5	3	20.64	3.46	415
D	1.1	1.1	0	21.12	2.64	380

getting diffused in the microcracking zone and macroscopic cracks. For example, the subsurface damage and cracks created by Knoop indentations on hot pressed Si_3N_4 specimens were viewed unambiguously after plasma etching.[18]

The purpose of this study is to investigate the mechanical response of ceramics by scratch testing in order to interpret their severe wear behavior. Hot pressed yttria stabilized α-SiAlON and α/β composite SiAlONs of various β-content were chosen as test materials in this study. Two types of stylus having different surface roughness were used for scratching in order to assess the variation in mechanical response of the material with surface integrity of stylus. Most reported works on scratch testing of ceramics have not discussed the dependence of results on the stylus surface roughness.[15,19–23] The extent of subsurface damage produced by the rough and smooth styluses beneath the sliding contact was visualized by plasma etching of taper-sections. The work required to produce the groove at a particular normal load (F_n) was investigated for various SiAlONs and results were correlated with their severe wear behavior.

2. Experimental procedure

2.1. Materials

Yttria stabilized SiAlONs of β-content varying from 0 to 50 vol.% were produced by hot pressed sintering. The chemical compositions of these materials are represented by $Y_{m/3}Si_{12-(m+n)}Al_{(m+n)}O_nN_{16-n}$, with $m = 0.5$ and $n = 0.25$ $m = 0.7$ and $n = 0.35$, $m = 1.0$ and $n = 0.5$, and $m = 1.1$ and $n = 1.1$, which were identified as 49%, 25%, 3% and 0% calculated β-content SiAlONs by XRD analyses. For simplicity, these test materials are hereafter, referred as materials A, B, C and D, respectively in this study. The processing, microstructure and mechanical and wear properties have been described in detail previously.[24] The mechanical properties and microstructures are reproduced here in Table 1 and Fig. 1, respectively. It should be noted that with increasing β-content in the materials there is a change in microstructure from one of equiaxed α-SiAlON grain morphology to one where elongated β grains uniformly are dis-

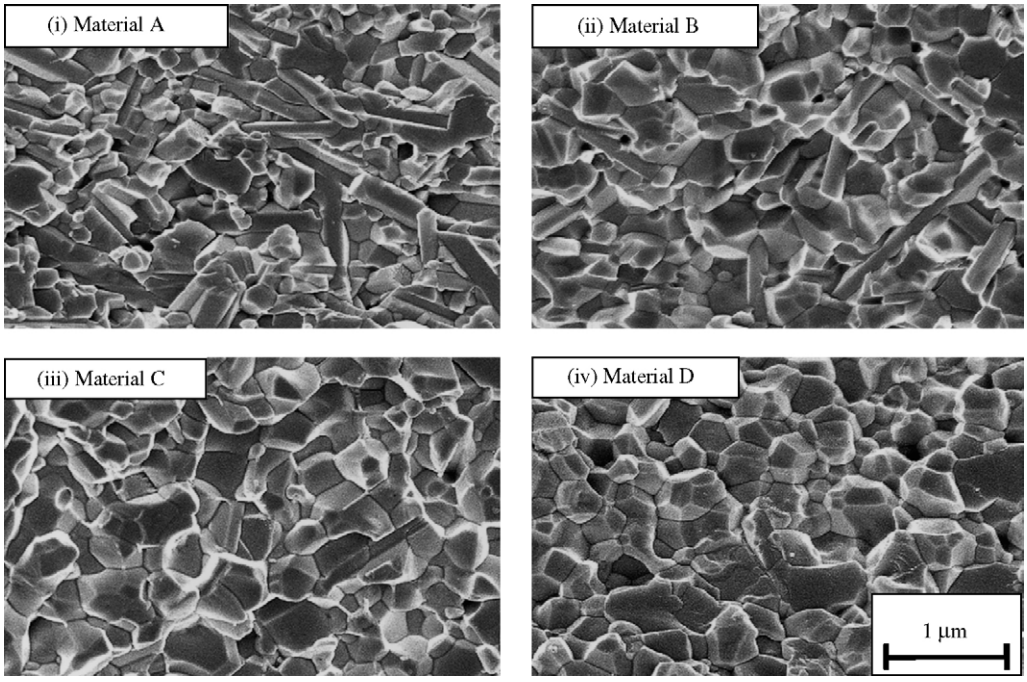

Fig. 1. Fracture surfaces of α/β-SiAlON composites (A) 50% β-content, (B) 25% β-content, (C) 3% β-content and (D) 0% β-content (pure α-SiAlON phase). Reproduced from Ref. 24.

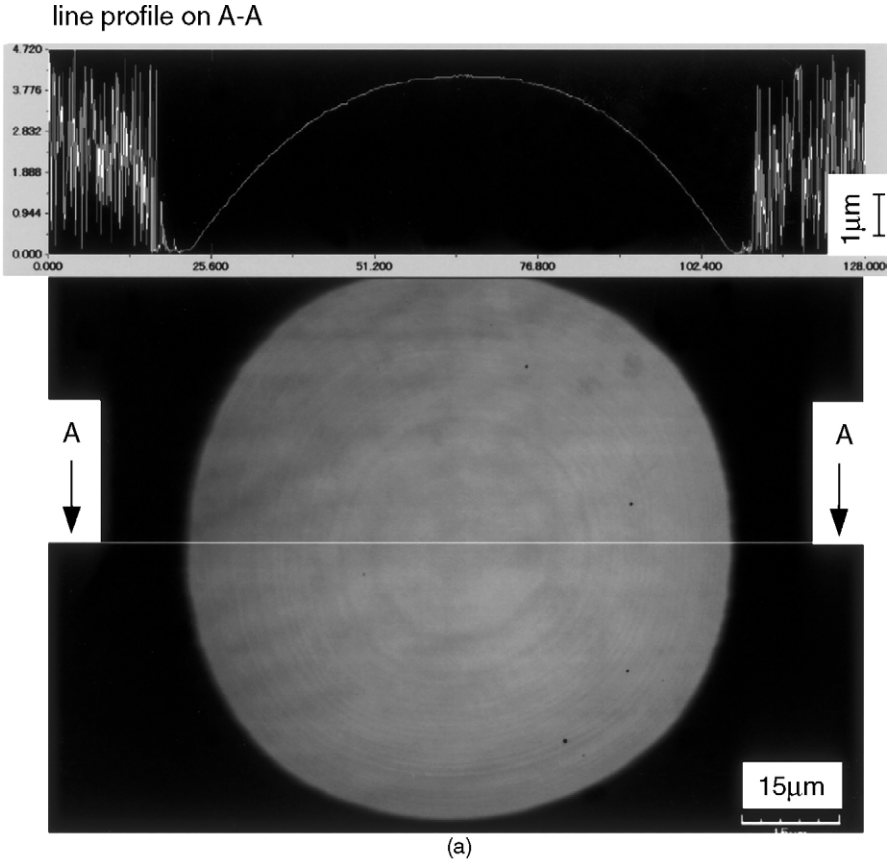

Fig. 2. Observations of (a) smooth stylus and (b) rough stylus taken by confocal laser microscopy, and surface profile of the rough stylus.

seminated in a fine α-SiAlON matrix. This leads to increased fracture strength as well as fracture toughness, whereas the hardness values decrease due to the lower hardness of the β phase.

2.2. Scratch tests

Scratch tests were conducted using a CSEM Revetest automatic scratch tester (CSEM, Switzerland) at room temperature and a relative humidity level range of 30% ± 5%. The specimens were cut from sintered disks and mirror polished using 0.5 μm diamond slurry for final finishing, resulting in a surface roughness of Rz less than 0.1 μm. Scratches were then performed on the polished surface with a spherical diamond stylus having radius of 200 μm and an apex angle of 120° at the spherical tip.

Two different types of stylus (NANOTEC, Japan) were employed, one is a smooth stylus with a mirror polished tip of low root mean square roughness (R_q = 0.47 μm) and the other is a rougher stylus with tip surface roughness of high R_q = 0.72 μm) specially designed for adhesion tests of hard coatings on metal.[25–27] Fig. 2 shows observations and line profiles of the two types of stylus taken by confocal laser microscope (OLS-1100, Olympus, Japan) prior to use. In the progressive loading scratch test with the smooth stylus, the nominal normal load was increased from 0 to a final maximum load of either 60 N or 70 N with a loading ramp of 300 N/min and a constant scratching speed of 30 mm/min. In the case of the rough stylus, the nominal normal load was increased from 0 to 17 N maximum with a loading ramp of 150 N/min and the same scratching speed. The normal load and its corresponding tangential force were recorded simultaneously during scratch tests. All test materials were scratched successively to identify the trend of tangential force with increased number of scratches at a constant maximum normal load. Scratch tracks were observed using an optical microscope in Nomarski illumination. Some of the scratched specimens were taper-sectioned across the scratch tracks with a taper angle of 3.5° to view the presence of damage beneath the sliding contact. Both scratch tracks and taper-sections underwent plasma etching in the following manner.

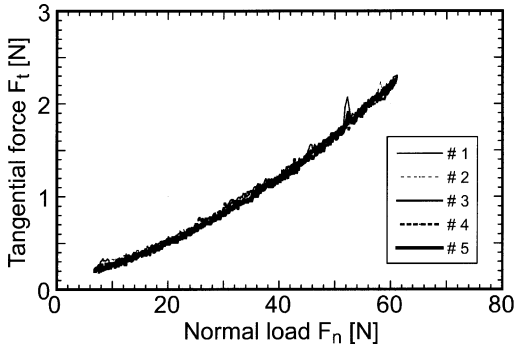

Fig. 3. Variation in tangential force F_t with normal load F_n for the first five scratches on material A with the smooth stylus.

2.3. Plasma etching

Plasma etching was carried out using a commercially available apparatus (EXAM El 106-E23, SHINKO SEIKI Co. Ltd., Japan), which is capable of generating power of 250 W maximum and operating with a radio frequency (RF) of 13.6 MHz. Reactive gas mixtures, containing CF_4 and 10% O_2 were used in plasma etching. A power of 60 W was applied during etching, previously optimized for uniform etching in preliminary studies. The etched specimens were rinsed ultrasonically in distilled water, where the water-soluble products formed, if any, can be removed. Etched surfaces were observed using an optical microscope in Nomarski illumination and/or SEM (FE-6330F, JEOL, Japan).

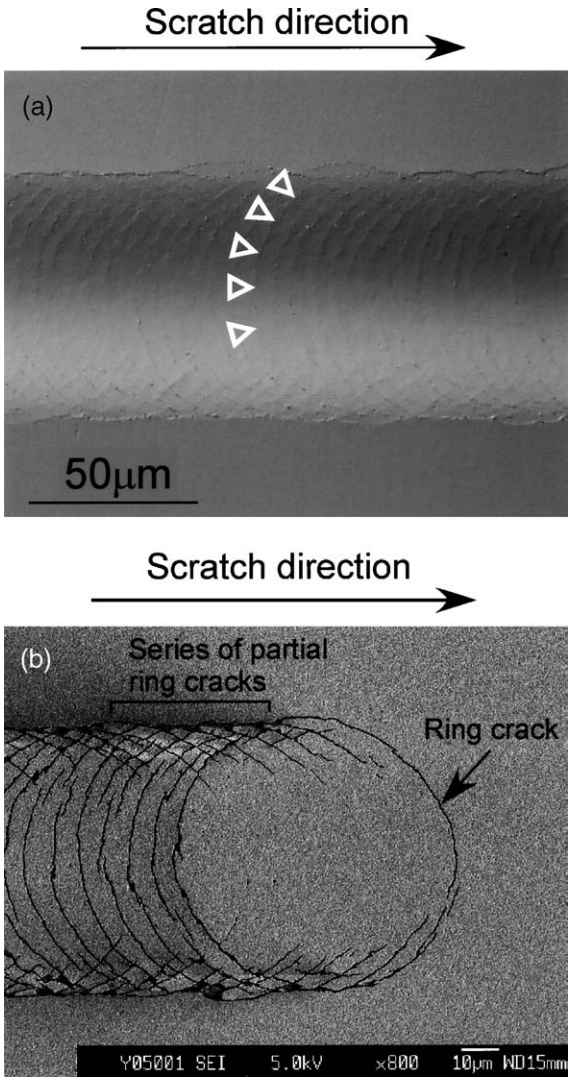

Fig. 4. Scratch groove on material A with the smooth stylus. (a) Optical microscopy image under Nomarski illumination before etching and (b) SEM image at the end of the scratch groove after etching.

3. Results and discussion

3.1. Scratches on material A by smooth stylus

The variation of tangential force (F_t) with normal load (F_n) for the first five scratches on material A by the smooth stylus to a maximum normal load of 60 N is shown in Fig. 3. F_n increased from 7 N to a maximum of 60 N and F_t increased monotonically with F_n. From the figure, it is seen that F_t, increased in an almost linear fashion at low normal loads, less than 20 N, and the slope of F_t increased with the increase in F_n at higher loads. It should be noted that there was very good reproducibility in results of F_t with increase in number of scratches.

The scratch grooves were observed using an optical microscope in Nomarski illumination before plasma etching and also using SEM after plasma etching and one of them is shown in Fig. 4a and b. The nominal normal loads corresponding to the center of the micrograph in Fig. 4a and scratch end in Fig. 4b are 60 N and 70 N, respectively. Before the etching, the presence of partial ring cracks is barely noticeable as indicated by triangles in Fig. 4a. Meanwhile, a series of partial ring cracks was distinctly visualized by etching as shown in Fig. 4b. These cracks are similar to partial cone cracks produced by spherical indenters on glass surfaces.[28]

To examine the presence of internal damage, a scratched specimen was taper-sectioned perpendicular to the scratch direction and the plasma etching carried out, as shown in Fig. 5. The damage can be easily observed under Nomarski illumination due to its sensitivity to slight height difference, whereas with SEM, delineation of the border between specimen surface and the taper-section is quite difficult due to the small taper angle. A darker area surrounded by triangles is evident in the interior of the section as shown in Fig. 5, implying the presence of quasi-plastic deformation. The depth from the surface was calculated from the angle of the taper and the distance between the taper edge and the point to be measured on the taper-section. A scale showing the depth from the scratched surface is given in the figure, and it can be seen that the subsurface damage could be observed at a minimum depth of approximately 3μm. This supports the result that the damage was invisible from the surface observations.

3.2. Scratches on material A by rough stylus

Material A was also scratched by the rough stylus to a maximum normal load of 17 N. The R_q of this stylus is almost 1.5 times that of the smooth one. The variation of F_t with F_n for the first five scratches is plotted in Fig. 6. The

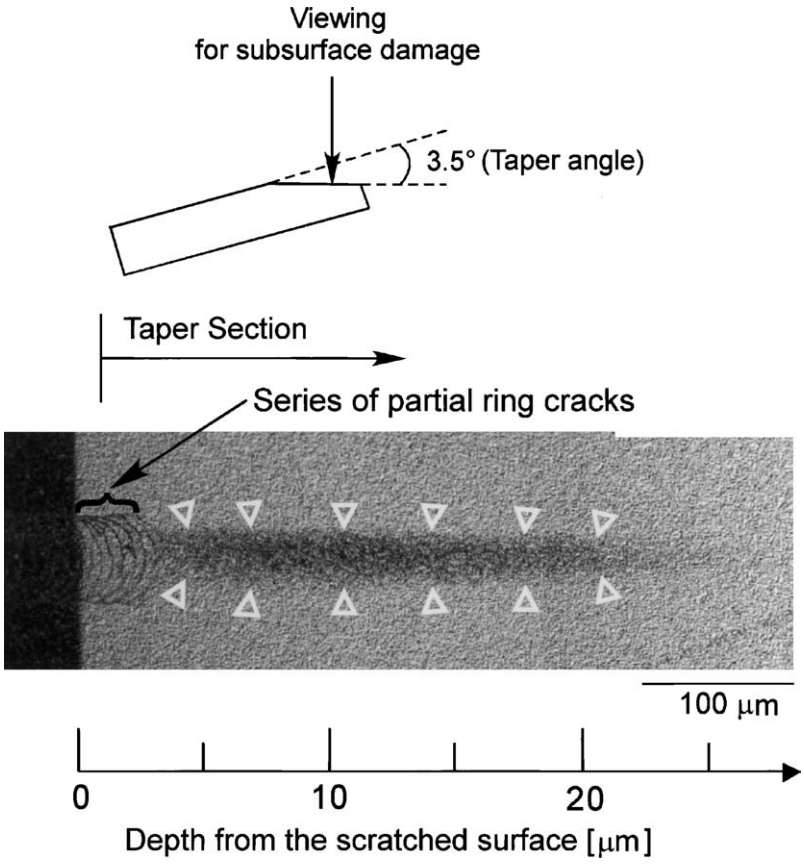

Fig. 5. Etched taper-section of the scratched specimen for subsurface damage observation. A series of partial ring cracks and damage in the internal area of the taper-section were clearly visualized after etching.

scratches started from a normal load of approximately 1 N to a maximum of 17 N with a steady increase of F_t with F_n. Unlike the smooth stylus, there was variation in the F_t versus F_n curves with increasing number of scratches. The cause of this variation will be discussed later.

Fig. 7 shows the observations of the scratched material by optical microscope under Nomarski illumination (Fig. 7a), and SEM following etching (Fig. 7b). The normal load applied at the center of each micrograph is 15 N and the scratch direction is from left to right in the figures. It is clear from Fig. 7a that the contact of the rough stylus is less uniform, thus producing an irregular profile to the scratch groove. This irregularity in the groove profile is due to asperities present on the rough stylus as shown in Fig. 2b. Fig. 7b demonstrates that the quasi-plastic deformation is predominant on the surface of specimen, which can be recognized as a region of grain release.[18]

The taper-section was examined for damage using optical microscopy in Nomarski illumination after plasma etching as shown in Fig. 8. The vertical dashed line in the figure shows the border between the specimen surface and the taper-section. From this figure, it can be seen that the quasi-plastic deformation is present in the subsurface, which is recognized as a dark region. The short arrows in the figure indicate the boundary of the quasi-plastic deformation on the taper-section. A series of arc cracks, highlighted by the triangles in the figure, were seen in the interior area of the taper-section, whereas the quasi-plastic deformation on the surface covered up the presence of arc cracks. The depth scale is attached in the figure and the depth of subsurface damage is approximately 1.6 μm.

Jones et al.[24] studied the wear response of these materials under dry sliding conditions and reported that worn surfaces of both α-SiAlONs and α/β-SiAlON composites (material D and A in our study) were very rough at high normal loads and material removal in the form of grain dislodgement from the surface occurred in this severe wear regime. This grain-dislodging phenomenon was reported to be due to intergranular cracks along the grain boundary in the subsurface region, which can lead to micro-fracture.[29] Considering the similarity of crack formation between grain dislodgement in wear and the subsurface damage during scratching, the scratch test with rough stylus is thought to be more appropriate than that of the smooth stylus for assessing and correlating the wear behavior of ceramics under severe wear conditions.

However, caution is required in correlating results of these two tests and to assure consistent results. The line profile of the rough stylus shown in Fig. 2, taken along the line B-B, which is perpendicular to the scratching direction, and the Nomarski illumination image of the scratched surface (Fig. 7) shows that non-uniform contact is obtained leading to a complicated stress state. For example, the contact stress at the asperity tips should be higher compared with the surrounding regions, in turn increasing the wear rate of the asperity. Hence, there is a possibility of a change in the profile of a stylus tip due to wear of asperities resulting in poor reproducibility in results. Further study is necessary to clarify the

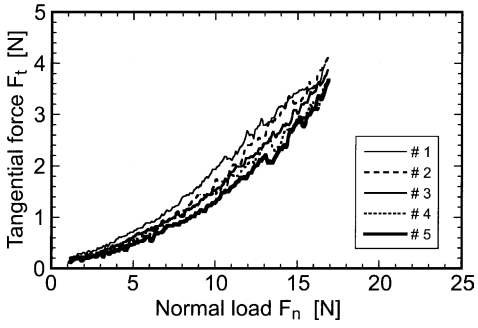

Fig. 6. Variation in tangential force F_t with normal load F_n for the first five scratches on material A with the rough stylus.

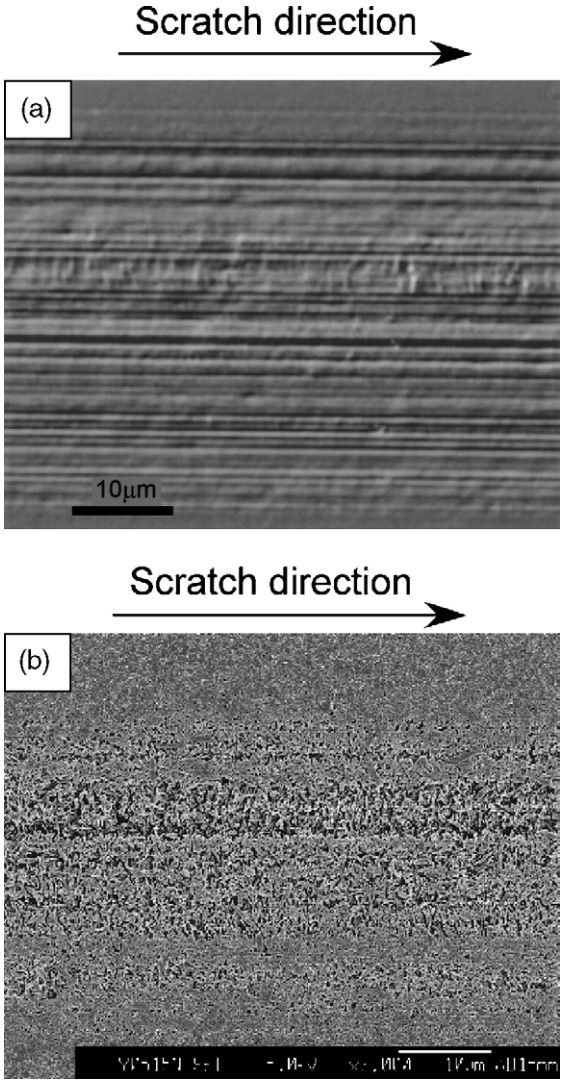

Fig. 7. Scratch groove on material A with the rough stylus. (a) Optical microscopy image under Nomarski illumination (b) SEM image after etching. Quasi-plastic deformation on the scratched surface was predominant after etching observed by SEM.

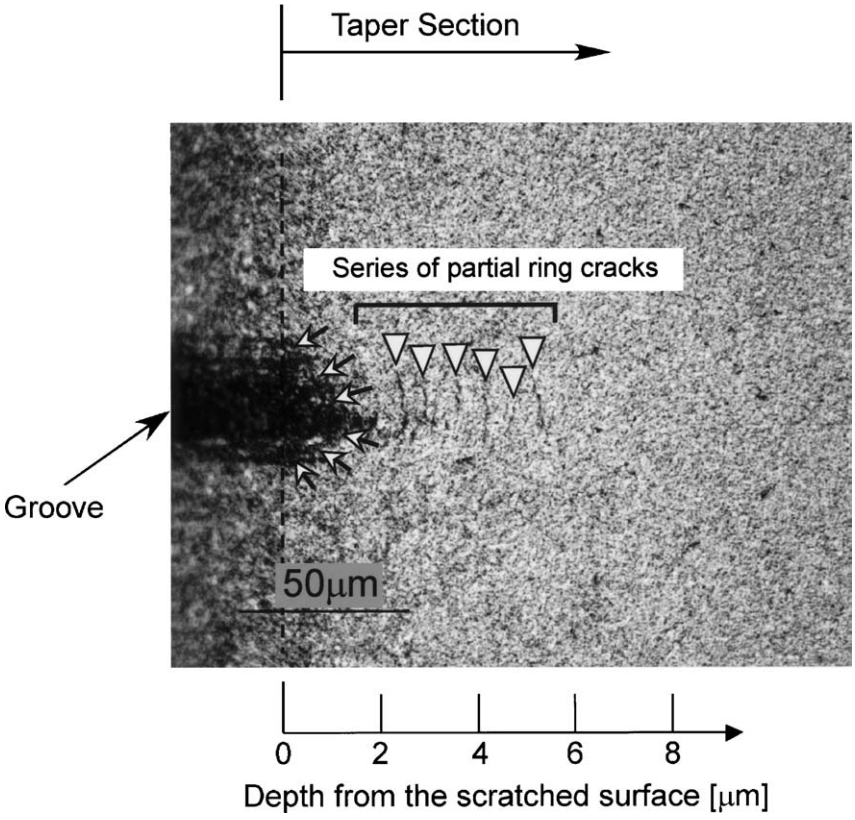

Fig. 8. Etched taper-section of the scratched specimen under Nomarski illumination. A series of partial ring cracks were noticed in the interior area of the taper-section.

cause of variation in the F_t versus F_n curves with number of scratches, but one could argue that F_t is very sensitive to the stylus and that F_t is dependent on the 'history' of the stylus in terms of factors, such as applied normal load and scratch length.

3.3. Scratches on various test materials by rough stylus

Repeated scratch tests were conducted for all the materials using the rough stylus. As was shown in Fig. 6 for material A, successive scratching resulted in a lower F_t for a given F_n, although the difference was low for the first five scratches. With a further increase in the number of scratches the difference in the curves becomes more obvious, but the curves return to their original levels when a new stylus is used. The same trend was observed for all materials and indicates that the "history" sensitivity mentioned above can be overcome by using a new stylus. In the following analysis, data from the first five scratches, using a new stylus is employed and the F_t against F_n curves are plotted in Fig. 9. For all materials, similar to material A, a trend of relatively smooth increase in F_t was observed with increase in F_n. As shown in Fig. 9, the dependence of F_t on F_n curves increases with increasing β-content in the materials (material A). The F_t versus F_n curves for the two α-SiAlON materials were superposed upon each other in the initial regions, and their magnitudes are smaller than that of the composites.

For all the test materials, the coefficient of friction (μ) was estimated by comparing the F_t to F_n ratio with scratch length for the averaged data of the first five scratches, as shown in Fig. 10 for the case of material A. In this figure, the ratio is almost constant up to a scratch length of around 0.7 mm. It is assumed that the mean value of ratio up to a scratch length of 0.7 mm (normal load of 4.6 N) indicates the sliding friction coefficient (≈0.11) prior to the onset of material removal by scratching. With further increase in sliding length, scratching

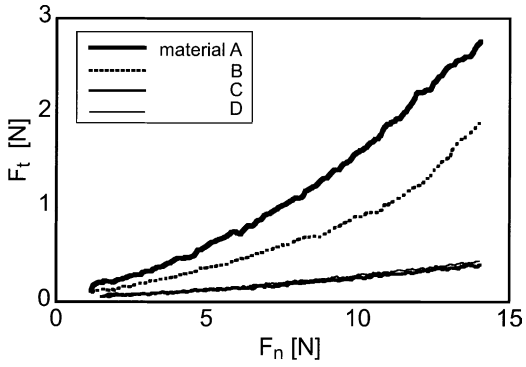

Fig. 9. F_t with F_n curves for all materials scratched with the rough stylus.

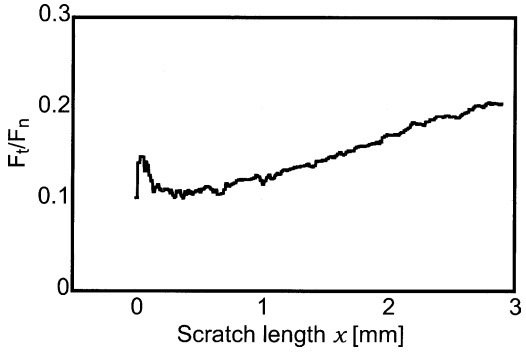

Fig. 10. Variation in the ratio of tangential force F_t to normal load F_n with scratch length for the mean data of the first five scratches on material A with the rough stylus.

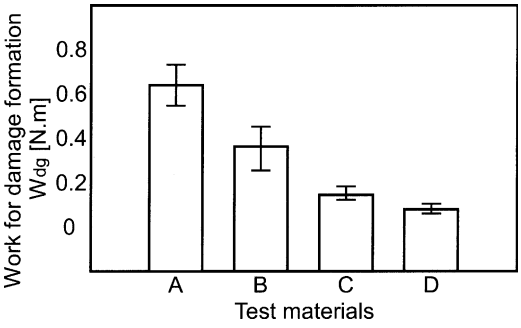

Fig. 12. Work required for damage and groove formation (W_{dg}) during scratching up to a constant normal load of 14 N for various SiAlONs, scratched with the rough stylus. The columns indicate the mean W_{dg} values of the first five scratches.

begins and the F_t to F_n ratio increased monotonically with scratch length. The initial fluctuations in the plot can be explained in terms of an unstabilized speed of the specimen table. The coefficient of friction was evaluated for other test materials in the same fashion. Fig. 11 shows the variation of F_t, whose scale is indicated on the left-hand scale, with scratch length for material A, where the data of F_t was averaged for the first five scratches. A linear relationship can be fitted to the initial portion of the curve. Meanwhile, the deviation of F, from the linear fitted line, $|\Delta F|$, can be determined by the absolute value of difference between the empirical fit and F_t,[22] i.e. $|\Delta F| = F_t - \mu F_n$. This value is also shown in Fig. 11 as the bold solid line. The onset of deviation of F_t was at a scratch length of 0.7 mm and correspondingly the $|\Delta F|$ had a steady increase with a further increase in the scratch length. The variation of $|\Delta F|$ with the scratch length was also determined for all test materials.

The work required for damage and groove formation (W_{dg}) can be calculated by measuring the product of $|\Delta F|$ and scratch length. In calculating W_{dg}, the friction coefficient used for determining $|\Delta F|$ was that determined as the sliding friction coefficient in the absence of material removal by scratching as described above, and assuming that there is no effect of change in stylus profile up to five scratches. The value of W_{dg} for the test materials calculated up to a normal load of 14 N, corresponding to a scratch length of approximately 2.6 mm, is plotted in Fig. 12. As was shown in Fig. 9, the curves of materials C and D were superposed upon each other in the initial region but there is a slight difference in W_{dg} due to difference in the curves at higher loads. In this figure the error bars show the spread of W_{dg} for the first five scratches with the maximum value corresponding to the first scratch and the minimum value corresponding to the fifth scratch. An increase in W_{dg} was observed with the β-content in α/β-SiAlON composites and material A had the highest W_{dg}. As it is assumed that the sliding friction coefficient in the absence of material removal by scratching is constant and that friction is low, it is thought that most of W_{dg} is consumed in the quasi-plastic deformation and cracking during the scratch tests. Consequently, the following hypothesis is suggested; Materials of high W_{dg} have high resistance to microcracking, and thereby, exhibit good performance in wear resistance. According to the wear tests results of Jones et al.,[24] the worn volume at severe wear conditions was highest for α-SiAlONs (material D, in our study) and least for 50% β-content SiAlON composites (material A). The worn volume of test materials under severe wear follows the reverse order of W_{dg}, which lends support to the suggested hypothesis.

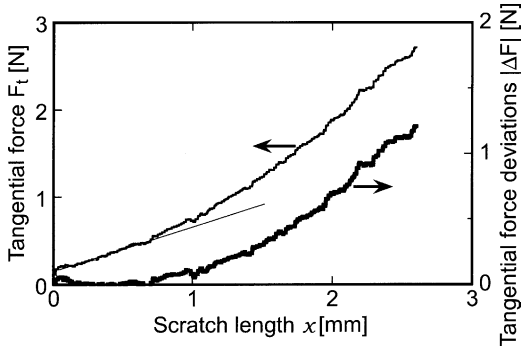

Fig. 11. Variation of tangential force F_t and the deviation in tangential force $|\Delta F|$ with scratch length for the mean data of the first five scratches on material A with the rough stylus.

4. Conclusion

Scratch tests were conducted for yttria stabilized α/β-SiAlON composites, where the β-content ranges from 0% to 50% in order to interpret the wear behavior of these materials under a severe wear regime. Two types of stylus having different surface roughness were used to assess the variation in mechanical response of material with surface integrity of stylus. Damage was observed by taper-sectioning the specimens across the scratches followed by plasma etching. When scratched by a smooth stylus, a series of partial ring cracks were formed on the specimen surface, but there was no quasi-plastic deformation present on the surface. However, when scratched by a rough stylus, the deformation was found predominantly on the surface, covering up arc cracks formed on the surface. Considering the similarity of crack forma-

tion between grain dislodgement during wear and subsurface damage in scratching, the scratch test with the rough stylus is more appropriate for comparing the two behaviors. The work required for damage and groove formation, W_{dg}, by the rough stylus was calculated for all test materials, and it was shown that this parameter follows the opposite trend to the worn volumes of these materials during severe wear. This supports the suggested hypothesis that materials with high W_{dg} have high resistance to microcracking and good performance in wear resistance.

Acknowledgments

Authors thank Mr. Hirotaka Tobita for his assistance in experiments.

References

1. Liu, W., Ye, C., Chen, Y., Ou, Z. and Sun, D. C., Tribological behavior of sialon ceramics sliding against steel lubricated by fluorine containing oils. *Trib. Int.*, 2002, **35**, 503–509.
2. Ravikiran, A. and Jahanmir, S., Effect of contact pressure and load on wear of alumina. *Wear*, 2001, **251**, 980–984.
3. Nakamura, M., Hirao, K., Yamauchi, Y. and Kanzaki, S., Tribological properties of unidirectional aligned silicon nitride. *J. Am. Ceram. Soc.*, 2001, **84**(11), 2579–2584.
4. Conway, J. C., Cohen, P. H. and Love, D. A., Dry sliding wear behavior of SiAlON ceramics. *Wear*, 1998, **126**, 79–80.
5. Cho, S.-J., Um, C.-D. and Kim, S.-S, Wear and wear transition mechanisms in silicon carbide during sliding. *J. Am. Ceram. Soc.*, 1995, **78**(4), 1076–1078.
6. Dong, X. and Jahanmir, S., Wear transition diagram of silicon nitride. *Wear*, 1993, **165**, 169–180.
7. Ravikiran, A. and Parimala Bai, B. N., Influence of speed on the tribochemical reaction products and the associated transitions for the dry sliding of silicon nitride against steel. *J. Am. Ceram. Soc.*, 1995, **78**(11), 3025–3032.
8. Gee, M. G. and Butterfield, D., The combined effect of speed and humidity on the wear and friction of silicon nitride. *Wear*, 1993, **162–164**, 234–245.
9. Krell, A. and Klaffke, D., Effects of grain size and humidity on fretting wear in fine grained alumina AI_2O_3/TiC and zirconia. *J. Am. Ceram. Soc.*, 1996, **79**(5), 1139–1146.
10. Kitaoka, S., Yamaguchi, Y. and Takahashi, Y., Tribological characteristics of α-alumina in high temperature water. *J. Am. Ceram. Soc.*, 1992, **75**, 3075–3080.
11. Dong, X., Jahanmir, S. and Hsu, S. M., Tribological characteristics of alpha alumina at elevated temperatures. *J. Am. Ceram. Soc.*, 1991, **74**(5), 1036–1044.
12. Gomes, J. R., Oliveira, F. J., Silva, R. F., Osendi, M. I. and Miranzo, P., Effect of α/β Si_3N_4—phase ratio and microstructure on the tribological behavior up to 700 °C. *Wear*, 2000, **239**, 59–68.
13. Skopp, A., Woydt, M. and Habig, K.-H., Tribological behavior of silicon nitride materials under unlubricated sliding between 22 °C and 1000 °C. *Wear*, 1995, **183–186**, 571–580.
14. Cho, S.-J., Moon, H., Hockey, B. J. and Hsu, S. M., The transition from mild to severe wear in alumina during sliding. *Acta Metal. Mater.*, 1992, **40**(1), 185–192.
15. Wang, Y. and Hsu, S. M., Wear and wear transition mechanisms of ceramics. *Wear*, 1996, **195**, 112–122.
16. Mikosza, A. G. and Lawn, B. R., Section-and-etch study of Hertzian fracture mechanics. *J. Appl. Phys.*, 1971, **42**, 5540–5545.
17. Kanematsu, W., Subsurface damage in scratch testing of silicon nitride. *Wear*, 2004, **256**, 100–107.
18. Kanematsu, W., Miyajima, T. and Sando, M., Visualization of Knoop indentation damage of silicon nitride by plasma etching. *J. Am. Ceram. Soc.*, 2001, **84**(10), 2427–2429.
19. Xu, H. H. K. and Jahanmir, S., Transitions in the mechanism of material removal in abrasive wear of alumina. *Wear*, 1996, **192**, 228–232.
20. Lee, S. K., Tandon, R., Readey, M. J. and Lawn, B. R., Scratch damage in zirconia ceramics. *J. Am. Ceram. Soc.*, 2000, **83**(6), 1428–1432.
21. Mukhopadhyay, A. K., Chakraborty, D., Swain, M. V. and Mai, Y.-W., Scratch deformation behaviour of alumina under a sharp indenter. *J. Euro. Ceram. Soc.*, 1997, **17**, 91–100.
22. Axen, N., Kahlman, L. and Hutchings, I. M., Correlations between tangential forces on the strength of brittle materials. *Trib. Int.*, 1997, **30**(7), 467–474.
23. Xie, Z. H., Hoffman, M., Moon, R. J., Munroe, P. and Cheng, Y. B., Scratch damage in ceramics: role of microstructure. *J. Am. Ceram. Soc.*, 2003, **86**(1), 141–148.
24. Jones, M. I., Hirao, K., Hyuga, H., Yamauchi, Y. and Kanzaki, S., Wear properties of Y-α/β composite sialon ceramics. *J. Euro. Ceram. Soc.*, 2003, **23**, 1743–1750.
25. Xie, Y. and Hawthorne, H. M., Wear mechanism of plasma sprayed alumina coating in sliding contacts with harder asperities. *Wear*, 1999, **225–229**, 90–103.
26. Xie, Y. and Hawthorne, H. M., Effect of contact geometry on the failure modes of thin coatings in the scratch adhesion test. *Surf. Coat. Technol.*, 2002, **155**, 121–129.
27. Ichimura, H. and Ishii, Y., Effects of indenter radius on the critical load in scratch testing. *Surf. Coat. Technol.*, 2003, **165**, 1–7.
28. Lawn, B. R., Wiederhorn, S. M. and Roberts, D. E., Effect of sliding friction forces on the strength of brittle materials. *J. Mater. Sci.*, 1984, **19**, 2561–2569.
29. Fischer, T. E., Zhu, Z., Kim, H. and Shin, D. S., Genesis and role of wear debris in sliding wear of ceramics. *Wear*, 2000, **245**, 53–60.